Magnetic Resonance Force Microscopy: Recent Results

C. S. Yannoni, O. Züger, K. Wago*, S. Hoen H.-M. Vieth ancl D. Rugar

IBM Research Division, Almaden Research Center, San Jose, California

Force detection of magnetic resonance has been demonstrated experimentally and used for imaging in EPR. This paper will review the basic principles of magnetic resonance force microscopy (MRFM) and will report some recent results in NMR imaging and the operation of a low-temperature MRFM.

I. Introduction

Since the discovery of electron paramagnetic resonance[1,2] and of nuclear magnetic resonance[3,4], EPR and NMR have become two of the most important spectroscopic tools in many areas, especially physics, chemistry, biophysics, biochemistry and materials science. Very detailed information at the molecular level can be obtained from ESR and NMR spectra, while magnetic resonance imaging (MRI)[5,6] is now routinely used by radiologists for clinical diagnosis. The reason that ESR and, in particular NMR, are so informative lies in their extremely high spectral resolution. A disadvantage of magnetic resonance, and especially NMR, is the low sensitivity of these methods due to the relatively low transition energies (4 x 10^{-5} eV for NMR and 10^{-2} eV for ESR) even at the highest polarizing fields currently available. As a result, samples containing at least 10^{15} nuclear spins or 10^9 electron spins are required for most NMR and ESR experiments, respectively. This limitation leads to a requirement for samples that are much larger than those used for studies by optical spectroscopy and restricts the investigation of surface and interface phenomena to materials with extremely high internal surface area. Therefore, the suggestion by Çidles[7] that it may be possible to detect a single nuclear spin was spectacular. Sidles proposed coupling the spin via magnetic force to a mechanical oscillator holding a field gradient source, a method that is very different from the inductive techniques used in conventional magnetic resonance. Reviews of the first theoretical and experimental work in magnetic resonance force microscopy (MRFM) have been written summarizing the progress made to date in demonstrating remarkable sensitivity for ESR and NMR[8,9].

A sketch of an idealized atomic-scale MRFM is shown in Fig. 1. The sketch shows that the MRFM is a magnetic force microscope[10] modified to do magnetic resonance experiments. The magnetic spins in the sample experience a force in the large gradient generated by a sharp magnetic tip attached to the cantilever. The force is given by

$$\mathbf{F} = (\mathbf{m} \cdot \nabla)\mathbf{B} , \qquad (1)$$

where m is the magnetic moment due to electron or nuclear spins and B is an inhomogeneous magnetic field. At resonance, the alternating magnetic field generated by the proximate coil causes a change in the force, which is detected with an optical fiber interferometer[11]. The gradient from the magnetic tip not only determines the strength of the force signal but, as in conventional magnetic resonance imaging, determines the spatial resolution of the MRFM. Nano-fabrication and chemical etching methods have demonstrated that it is possible to produce tips with a radius of curvature of 300Å,

[12] which would generate magnetic field gradieiits as large as 100 gauss/Å (10^8T/m). Therefore, even if all tlie spins shown in Fig. 1 were identical, it should be possible, using sucli high gradients, to excite one spin at a time, permitting direct atoin-by-atom imaging of molecules. MRFM thus has the potential for atomic-scale microscopy witli elemental specificity. Although such a capability may be difficult to achieve, the experiments reported here show tliat micron-scale ESR[13,14] and NMR[15] images have already been obtained using MRFM. Good agreement between tlie estimated and observed spin sensitivity in tlie MRFM results reported to date suggest that the detection of a single electron spin is a realistic possibility[8]. In tliis paper, basic principles of MRFM are reviewed, and some recent results in NMR detection and imaging are reported.
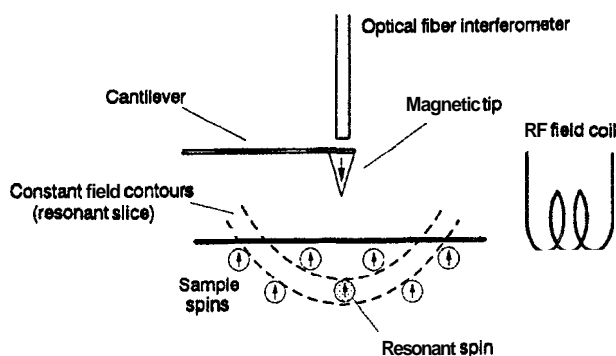

Figure 1. Sketcli of a proposed magnetic resonance force microscope witli atomic resolution. The gradient of tlie field produced by the nanoscale-size magnetic tip is strong enough to isolate a single electron or nuclear spin. Tlie rf coil is used to excite the rnagnetic resonance.

II. Basic principles of the MRFM

The basic detection principle of MRFM is to couple the motion of spins to the motion of a meclianical cantilever and to monitor the position of tlie caiitilever. A sketcli of tlie probe that was used to do tlie first force-detected NMR experiment[16] is shown in Fig. 2[17]. It should be noted tliat tlie sample, ratlier tliaii tlie magnetic tip, is mounted on tlie cantilever. Tliis configuration was necessary due to tlie large size of the magnetic tip used as a gradient source in these experiments[18]. If the force on the spins in the sample can be modulated at the cantilever frequency, f_c, tlien an enhancement of the amplitude of deflectioii of the cantilever can be realized:

$$A = (Q/k)F \qquad (2)$$

wliere A is the deflection amplitude of tlie cantilever, Q is the quality factor of tlie cantilever oscillator and k the spring constant of the cantilever. F is amplitude of the oscillatory force on tlie spins in the gradient generated by the magnetic tip. From an analysis of the noise (see section V), a major goal in the design and construction of cantilevers is achieving a high Q and low force constant. This is most effectively realized by fabricating small, and, in particular thin cantilevers to be used iii a modest vacuum (10^{-4}Torr)[16,19]. For very small, light cantilevers witli low force constant, typical cantilever frequencies are ≤ 100 kHz[19]. These frequencies are orders of magnitude lower than the Larmor frequencies used iiowadays in magnetic resonance (as high as 750 MHz for protons and 250 GHz for electrons).
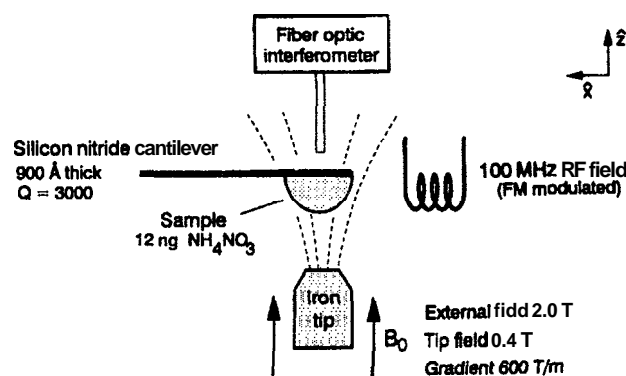

Figure 2. Sketcli of tlie force detection apparatus used to detect NMR. In this configuration, the sample is mounted on tlie cantilever. The tip which generates tlie field gradient can be translated to sweep tlie field through the resonance condition. The position of the cantilever is monitored with a fiber optic interferometer.

The spin dynamics relevant to MRFM and conventional magnetic resonance experiments are thus very different. The spin system in a sample in a magnetic field oriented along the z axis is characterized by a magnetic moment m $= M_z V$, where M_z is the Curie spin magnetization and V is the sample volume. In tlie MRFM experiments performed to date, M_z is forced to vary slowly at frequencies $\sim f_c$, in contrast to conventional magnetic resonance, where the transverse magnetization $M_{x(y)}$ rotating at the Larmor frequency is detected. Since M_z is the projection of the spin magnetization, $\mathbf{M}_0$, along the z-axis, a change in either the

magnitude or direction of M_0 will result in a corresponding change in M_z and in the force on tlie spins of the sample mounted on tlie cantilever. Tlie vibration of the cantilever can be excited by modulating tlie magnitude or direction of M_0 at f_c, resulting in a time-varying force. The change in amplitude of the cantilever vibration is then registered by the fiber optic interferometer.

III. Summaãy of first results

1. Force Detectioii of ESR[20]

Cyclic saturation[21] was used to change tlie magnitude of M_0 for force detection of ESR. Tliis was accomplished by modulating tlie dc field through resonance, resulting in cyclic saturation of M_0, and a corresponding reduction in M_z. A calculation of this effect is shown in Fig. 3(top); since M_z is reduced twice each modulation cycle, a second-harmonic response [Fig. 3(bottom)] can be detected. Detection at the second harmonic circumvented interfereiice due to spurious feed-through at tlie fundamental frequency. The first experimental result in MRFM[20], tlie ESR spectrum of 30 nanograms of DPPH, is sliown in Fig. 4(a); for comparison, a theoretical calculation of tlie expected force-detected signal is shown in Fig. 4(b). Tlie only free parameter in tliis calculation is the streiigtli of the rf field used to saturate the electron spiiis. A requirement for tliis experiment to work is tliat tlie electron spin-lattice relasation time (T_{1e}) be sliort compared with the cantilever period. Since f_c was 4 kHz, and T_{1e} in DPPH is 60 naiioseconds, tliis condition was easily fulfilled. Sidles aiid co-workers have proposed and demonstrated the utility of anharmonic modulation for ESR force detection of DPPH, and have sliown that this method suppresses noise and feed-through[22].

2. Force-detected ESR Imaging[13,14]

The detection teclinique described above was used in imaging two micron-sized particles of DPPH by mounting the gradient source on a movable x-y-z piezoelectric stage and gathering two-dimensional (x-y) data. This was done for the axial direction (z) defined by the axis of the gradient source, a conical piece of NdFeB[13]. The axial and lateral gradients were 4.3 G/μm and 0.94 G/μm, respectively. As the tip is scanned, tlie mag-

nitude of tlie spin magnetization in the DPPH particles will become cyclically modulated when the field at tlie particle lias tlie resonance value B_0 and the corresponding change in force will be detected using the method described above. The spatial variation of the field generated by a conical tip is shown in Fig. 5(a), and tlie surface of constant. field strength is approximately a paraboloid. For the point sample shown in Fig. 5(a), a scan of the tip in the x-y plane at $z = z_2$ will generate a circular force "map" indicating where tlie magnetic resonance condition is met on the surface $B_t(x,y,z) = B_0 = $ const. Typical force maps demonstrating tliis behavior for different distances from the tip are sliown in Fig. 5(b). A photomicrograph of tlie two DPPH particles glued to the silicon nitride cantilever[23] is shown in Fig. 6(a), and a force map generated as described above is shown in Fig. 6(b). An ESR image of tlie two DPPH particles reconstructed froin tlie force map of Fig. 6(b) using conventional image reconstruction tecliniques is shown in Fig. 6(c)[14]. Comparison of Figs. 6(a) aiid (c) shows tliat the ESR image reproduces tlie shape and dimensions of the DPPH particles very well. Tlie spatial resolution in the asial and lateral directions was 1.2 pm and 5.3 pm, respectively.
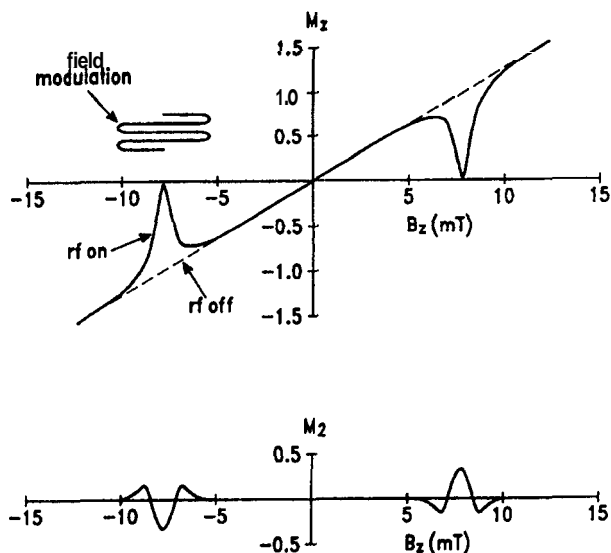

Figure 3. Top: calculation of the beliavior of tlie longitudinal spin magnetization, M_z, as a function of external magnetic field with (solid curve) and without (dashed curve) rf irradiation. M_z is suppressed at magnetic resonance; bottom: second harmonic response of the change in M_z produced by modulating the dc field.
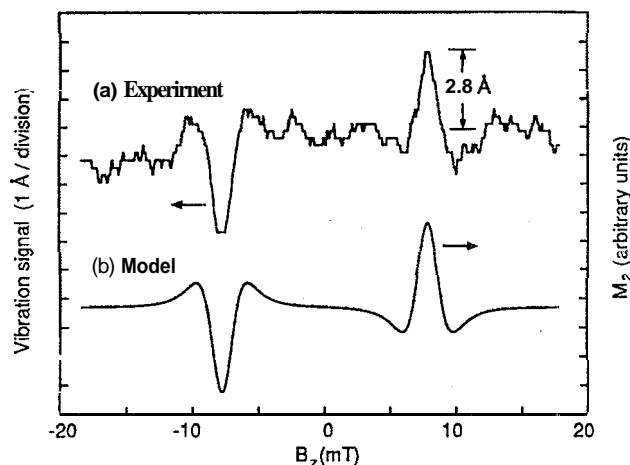
Figure 4. (a) amplitude of cantilever vibration measured at tlie second harmonic of tlie modulation frequency plotted as a fuiiction of tlie polarizing fielcl for a peak modiilation amplitude of 1 mT and rf excitation at 220 MHz. Vibration peaks occur at field values corresponding to electron spin resonance in diphenylpicrylliydrazyl (DPPH). (b) calculation of tlie second liarmonic response using known experimental parameters with tlie exception of tlie strengtli of tlie rf field, $B_1 = 3.4$ mT, which was chosen to give the best fit with the data in (a).
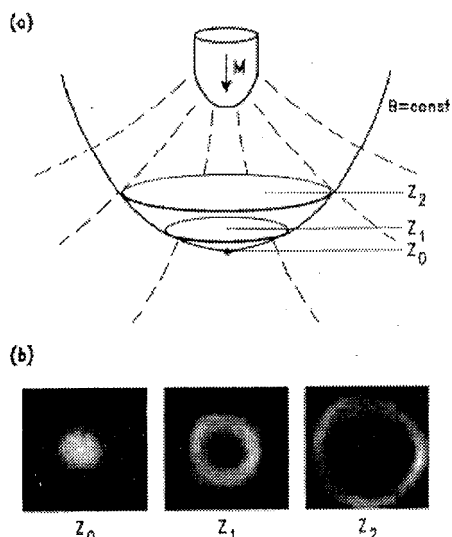

Figure 5. (a) dashed lines show tlie magnetic field lines from tlie tip used for EPR imaging. The surface of constant field strengtli is a paraboloid and the circles indicate where the magnetic resonance condition is met on tlie surface $B = B_0 = $ const. as the tip is scanned in tlie x-y plane at a fixed sample distance, z, from the tip. (b) force maps measured for a small DPPH particle scanned in the x-y plane at three different values of $z : z_0 \simeq 200\mu$m, $z_1 = z_0 - 3\mu$m, $z_2 = z_0 - 8\mu$m. The gray scale represents cantilever vibration amplitude, with white representing maximum amplitude. Tlie image size is $200 \times 200\mu$m^2.
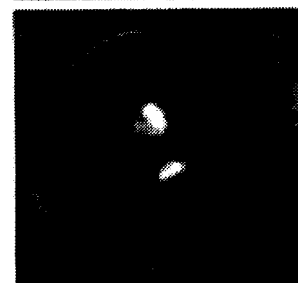

(a) Sample
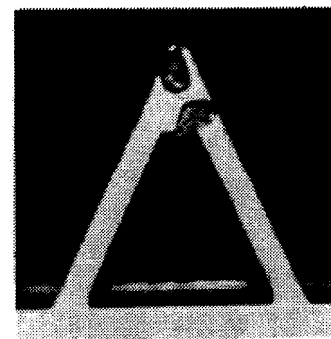
(b) Force map

(c) Reconstructed image

50μm

Figure 6. (a) optical micrograph showing two DPPH particles attached to a silicon nitride cantilever; (b) magnetic resonance force map (*vide infra*) of the sample, consisting of a 128 x 128 pixel array acqiiired during a 90-minute scan; (c) reconstructed electron spin density image obtained by deconvolving the data in (b); tlie large rings slightly visible in the image are artifacts of tlie deconvolution procedure.

3. Force Detection of NMR[16]

Force detection of NMR presented a major challenge since (1) the magnetic moment of nuclei is $\sim 10^3$ times smaller than the electron spin moment and (2) the shortest spin lattice relaxation times for nuclei are a few hundred μs so that the use of the cyclic saturation technique described above for ESR is precluded. In order to overcome these difficulties, very sensitive cantilevers were fabricated[19], a high external field was used to increase the nuclear spin polarization and cyclic adiabatic reversal[24] was used to change the direction of tlie nuclear magnetic moments at $f_c^{[16,25]}$. A photo-

900Å Thick Silicon Nitride Cantilever
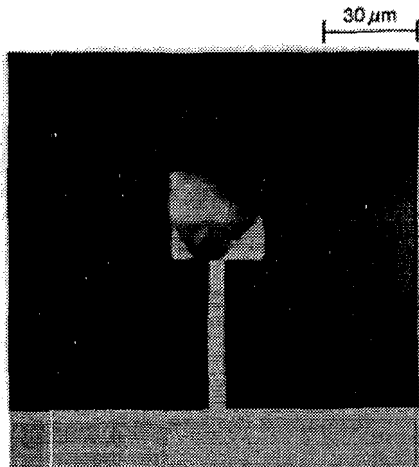
- $k = 10^{-3}$ N/m
- $Q = 3000$ in vacuum
- 5×10^{-16} N/$\sqrt{Hz}$ force sensitivity at 300 K.

Figure 7. Optical micrograph of the 900 Å-thick silicon nitride cantilevei, with a 12-nanogram grain of ammonium nitrate mounted on the paddle-shaped end.

micrograph of a 900Å -thick cantilever holding a 12-nanogram sample of ammonium nitrate is shown in Fig. 7[16]. The loaded cantilever, fabricated from silicon nitride[19], resonates at 1.5 kHz, with Q = 3000 and $k = 10^{-3}$ N/m. The achieved force sensitivity was 5×10^{-16} N in a 1 Hz bandwidth at 300K (see eq. **3** in section V). The rf frequency modulation sequence used to generate cyclic adiabatic reversal of the protons is shown in Fig. 8. After allowing sufficient time for the protons to polarize in the external field ($\sim$4 s), the rf field is turned on far off resonance (to avoid saturation of the protons), and the frequency is then swept adiabatically through resonance and modulated back and forth across the resonance value at a frequency $f_c = 1.5$ kHz. This foices the proton magnetization to change its direction with respect to the external field direction (z) at f_c, and produces enhancement of the cantilever deflection given by eq. 2. The change in proton magnetization generates an alternating force which drives the vibration of the cantilever, monitored by the interferometer (Fig. 2). Force detection of the proton **NMR** in ammonium nitrate is shown in Fig. 9, in which the cantilever vibration amplitude is plotted against time while the rf srquence shown in Fig. 8(a) is applied.

The single-shot sensitivity at ambient temperature in a field of 2.35T (100 MHz proton NMR) is 1.6×10^{13} spins. This sensitivity is about three orders of magnitude higher than conventional solid state NMR methods.
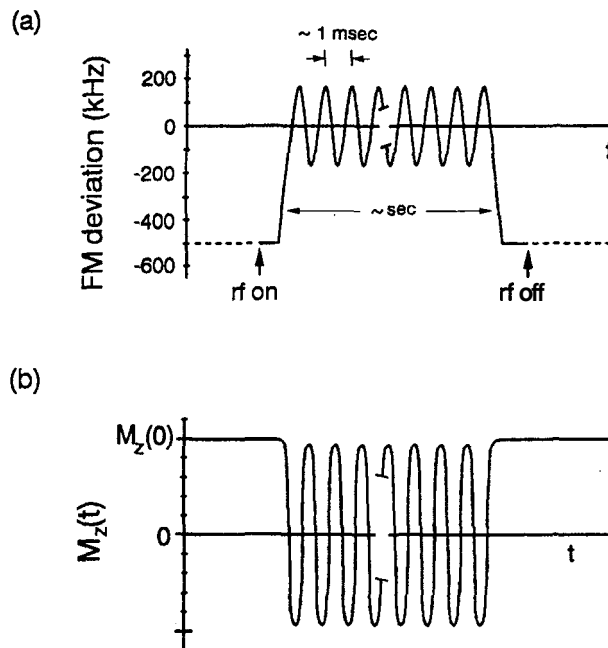
(a)

(b)

Figure 8. (a) frequency modulation sequence used for cyclic adiabatic inversion showing the rf frequency deviation $\Omega(t)/2\pi$; (b) time dependence of the longitudinal magnetization (M_z) resulting from the sequence in (a).
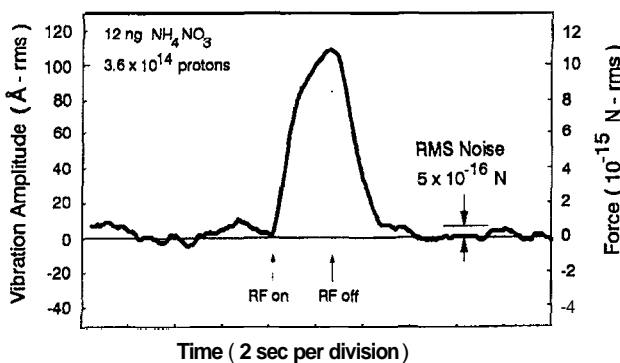

Figure 9. Force detected NMR signal of the protons in a 12 nanogram sample of ammonium nitrate. The sequence shown in Fig. 8(a) was turned on and off as indicated and the cantilever vibration amplitude measured at the fundamental cantilever frequency during this single-shot experiment (no averaging). The slow rise and fall times of the response are primarily a result of the 1 s time constant of the lock-in amplifier. Measurement conditions: rf field strengtli (B_1) = 12 G, $\Omega/2\pi = 170$ kHz and $Q_{eff} = 1000$[15].

The force detection method has also been used to measure the proton T_1 and to observe transient

nutations of tlie proton magnetization[26]. A one-dimensional image of the ammonium nitrate sample was obtained and a resolution of $\sim 2.6\mu$m estimated[16]. The following section describes three-dimensional imaging of the protons in an ammonium nitrate crystal.

IV. Three-dimensional proton imaging[15]

Three dimensional proton imaging was carried out using tlie NMR force detection method describecl above[15]. Tlie gradient source, a ferromagnetic tip (0.25 inm diameter iron wire, 4 min long), was inounted on piezoelectric translators for motion in tlie x aiid y directions as shown in Fig. 10. Tlie field at tlie sample is tlie sum of the homogeneous field froin the superconducting magnet and tlie tip fielcl. Tlie field from tlie tip decreases as tlie distance from tlie tip increases. Therefore, by varying tlie rf frequency, w, protons at different depths of tlie sample aloiig a direction (z) defined by the axis of tlie cylinder, can be excited. Iii order to acquire tlie data for a 3-dimensional iinage, the tip is kept at a constant distance from tlie sample and scanned in tlie x-y plane and tlie rf frequency is scaiined over a range Sw. Tlius, an $x - y - $ w lattice of 31 x 31 x 50 points was generated. Tlie x and y coordinates range over 100 pm, wliile w was clianged from 96.3 MHz to 101.2 MHz. A range of $\delta\omega$ corresponds to a distance $\delta z = \delta\omega(\gamma G_z)^{-1}$, wliere G_z is tlie gradient iii tlie z direction. Since tlie z-gradient was 22 gauss/μm witli tlie tip positioned 150 μm from tlie sample, tlie w scan was equivaleiit to a z-scan of 52 pin. At eacli lattice point, tlie response of the cantilever was measured while the excitatiori sequence sliowii iii Fig. 8(a) was applied. Fig. 11 shows $x - \omega$ force maps for four of the 31 different y positions. Tlie paraboloidal sliape of the tip field profile is clearly reflected by tlie force maps. Tlie force inaps reflect tlie amplitude of tlie first harmonic response of tlie caiitilever to tlie time-varying force imposed by modulation of tlie magnetization of tlie protons that are excited. Tlie image of the sample consists of spatial variation of the proton density which can be deconvolved from the force maps witli a knowledge of the spatial variation of tlie external magnetic field and the field gradient from the iron tip. The deconvolution was performed using a Wiener filter[14].

1. Results and Spatial Resolution

A surface of constant proton density in an ammonium nitrate crystal ohtained using this metliod is showii in Fig. 12. Tlie flat part of tlie side view, parallel to tlie plane of the cantilever, represents the surface of tlie crystal facing the cantilever. The overall shape and climensions of tlie surface shown in Fig. 12 closely reproduce an optical image of the sample. The spatial resolution of this method can be determined experimentally from relevant features of the proton spin density reconstructed from force maps. The resolution acliieved in the axial direction was **3.6** μm and 17.5 μm in tlie lateral direction, yielding a volume resolution of $(10\mu$m$)^3$. Volume resolution of $(10\ \mu$m$)^3$ is three orders of magnitude greater than proton imaging in solids using conventional methods[27], and at the limit of volume resolution *calculated* theoretically for solution proton imaging[28]. Higher spatial resolution and sensitivity is expected of MRFM with the use of larger field gradients and more sensitive cantilevers.
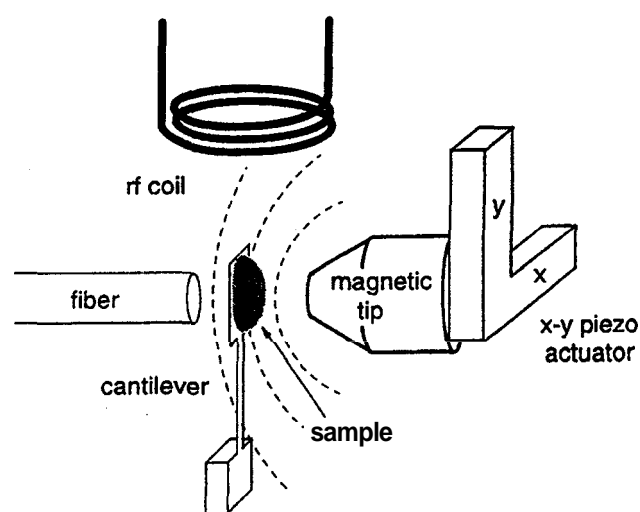

Figure 10. Schematic view of the NMR force microscope. Tlie dashed lines represent contours of constant magnetic field.
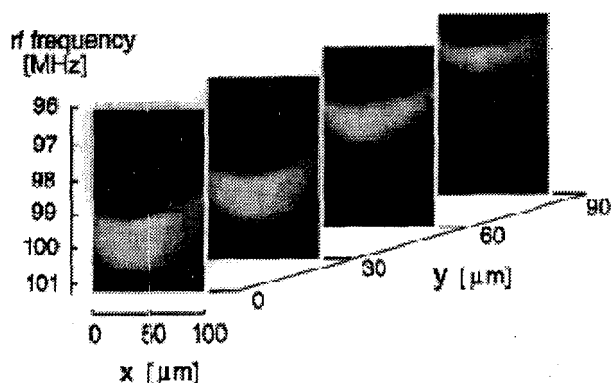
Figure 11. Three-dimensional force map of the sample obtained by scanning the rf frequency for each x-y position of the magnetic tip, moved by piezoelectric actuators over a 100 μm range. The conversion factor is 10.5 μm/MHz.

V. Low Temperature MRFM Detection of ^{19}F NMR[29]

Force sensitivity in MRFM is limited only by thermal cantilever noise. The minimum detectable force is[30,31]

$$F_{\min} = (2kk_BT\Delta\nu/Q\pi f_c)^{1/2} , \qquad (3)$$

where k_B is the Boltzmann constant, T is the temperature and Av is the detection bandwidth (Hz). It is clear from eq. 3 that low-temperature operation should increase the sensitivity of the MRFM. An additional advantage is that the magnetic moment due to spin polarization, which is inversely proportional to temperature, will also increase, resulting in a larger force signal (eq. 1).

1. Experimental details

The MRFM was suspended in a vacuum can to provide vibration isolation and cooling was achieved by heat-sinking the cantilever mount to the bottom of the can via copper braid. The can was immersed in the liquid helium bath of a cold-bore superconducting magnet used to generate an external magnetic field. The field gradient source, a cylindrical iron tip 1.5 mm diameter x 3 mm long, generated a gradient of 6 gauss/μm and an additional field of 0.41T at a distance of 600 μm to 700 μm from the sample. The cantilever, commercially fabricated from single crystal silicon, was 470 μm long by 45 μm wide by 1.5 μ thick, with L = 0.07 N m^{-1}, f_c = 9.8 kHz (without sample) and Q = 4 x 10^4 at room

temperature in the vacuum of 10^{-5} Torr. The effect of temperature on the thermal noise is shown in Fig. 13. The vibration amplitude of the cantilever measured at the resonance frequency was 1.1 A-rms at room temperature (Fig. 13a) and decreased to 0.26 Å-rms at 6K (Fig. 13b); the cantilever Q also increased to 2×10^5 at this temperature. The minimum detectable force at 6K was estimated to be 8 x 10^{-17} N/(Hz)$^{1/2}$, about twice the expected theoretical value. The discrepancy may be due to some environmental noise resulting from incomplete vibration isolation.
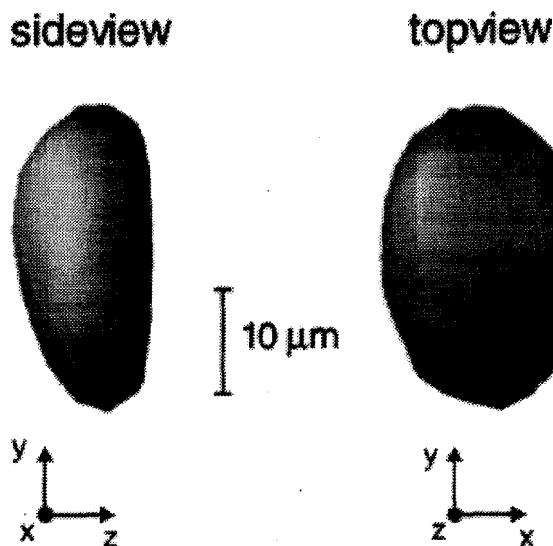

Figure 12. Reconstructed proton spin density of the ammonium nitrate sample, showing a constant density surface. The reconstruction was obtained from the force map in Fig. 11 by a deconvolution technique. The flat part in the side view represents the surface of the sample facing the cantilever.

2. Results

The first low-temperature force-detected magnetic resonance spectrum, the ^{19}F NMR spectrum in calcium fluoride (CaF$_2$) doped (1%) with Nd^{+3} ions, is shown in Fig. 14. The experiment was carried out at 14K in a dc field of 2.55T with an rf field strength of 19 gauss at 102.8 MHz, a (loaded) cantilever frequency of 1.6 kHz and a peak modulation amplitude of 280 kHz, equivalent to 70 gauss for ^{19}F. A special excitation sequence designed to circumvent the rapid decay of the ^{19}F magnetization during the cyclic adiabatic reversal sequence was used[26]. The ^{19}F lineshape can be interpreted as a one-dimensional spatial map of the spin density projected onto the z axis, which is the symmetry axis of

tlie cylindrical iron tip. Since tlie field gradient produces different polarizing fields in differeiit z positioiis of tlie sample, successive x-y slices of tlie sainple come into resonance as tlie dc field is scannecl, generating a. magnetic force proportional to tlie number of ^{19}F spins within tlie slice. Tlie observed ^{19}F linewidtli of 500 gauss in tlie gradient of 6 gauss/μm corresponds to a sainple tliickness (z direction) of $\sim 80\mu$m.
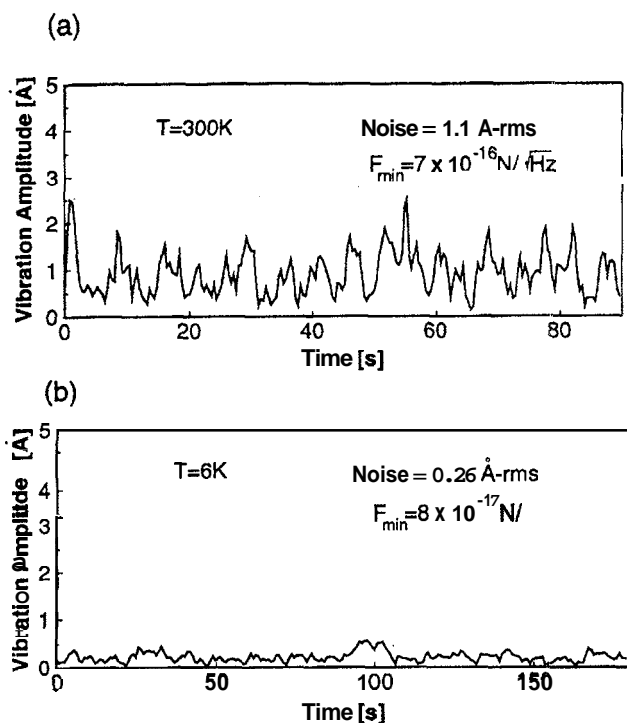
(a)

(b)

Figure 13. Vibration noise of tlie cantilever optically monitored at tlie resonant frequency (9.8 kHz) at (a) 300K and (b) 6K.
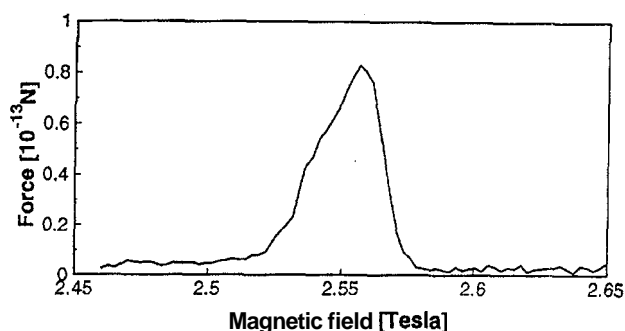

Figure 14. Tlie NMR force signal of ^{19}F in 1% Nd-doped CaF_2 measured at 14 K a.s a function of polarizing fielcl.

VI. Summary and Conclusions

Tlie relatively brief history of MRFM has been summarized here witli the following conclusions: MRFM

has been cleinonstrated experimeiitally for (1) the detectioii of both ESR and NMR with high sensitivity; (2) ESR imaging with resolution of $\sim$ 1pm; (3) NMR imaging witli volume resolution of $(10 \ \mu$m$)^3$; (4) MRFM at low temperatures, witli nearly tlie expected increase in sensitivity as thermal cantilever noise is decreased. Tlie ultimate goal of tliis work, as stated in tlie Introduction, is to develop a inicroscope that can detect the NMR of individual atoins with three-dimensional sub-Ångstrom spatial resolution. Apart from intrinsic value as a scientific tool, an atomic MRFM would have a broad range of applications in molecular biology, materials and polyiner science, surface science and nanotechnology. In order to achieve this goal, considerable innovation will be required in a number of areas and in particular in cleveloping improved sensors to detect extremely small forces and new methods for manipulating nuclear spins. Theoretical treatments of force signal and noise and of inagnetic resonance, which have describecl closely the results obtained to date and provide a reliable basis for predicting tlie results of future experiments, encourage a sustained effort to develop MRFM with atomic resolution.

References

1. E. K. Zavoisky, J. Pliys. USSR 9, 211 (1945).
2. E. K. Zavoisky, J. Pliys. USSR 9, 245 (1945).
3. E. M. Purcell, H. C. Torrey and R. V. Pound, Pliys. Rev. 69, 37 (1946).
4. F. Blocli, W. W. Hansen aiid M. Packard, Phys. Rev. 69, 127 (1946).
5. P. Lauterbur, Nature 242, 190 (1973).
6. P. Mansfield and P. K. Grannell, J. Pliys. C.: Solid State Pliys. 6, L422 (1973).
7. J. A. Sidles, Appl. Phys. Lett. 58, 2854 (1991).
S. J. A. Sidles, J. L. Garbini, K. J. Bruland, D. Rugar, O. Zuger, S. Hoen and C. S. Yannoni, Rev. Mod. Pliys. 67, 249 (1995).

9. C. S. Yannoni, O. Zuger, J. A. Sidles and D. Rugar, in *Encyclopedia of Magnetic Resonance*, edited by D.M. Grant and R.K. Harris (Wiley, Sussex, 1996).

10. P. Grütter, H. J. Mamin ancl D. Rugar, in *Scanning Tunneling Microscopy II*, edited by R. Wieseiiclanger and H.-J. Güntherodt (Springer-Verlag, Berlin, 1992), p. 151.

11. D. Rugar, H. J. Mamin ancl P. Guethner, Appl. Pliys. Lett. 55, 2588 (1989).

12. D. Rugar, H. J. Mamin, P. Guethner, S. E. Lambert, J. E. Stern, I. McFadyen and T. Yogi, J. Appl. Phys. 68, 1169 (1990).

13. O. Zuger and D. Rugar, Appl. Pliys. Lett. 63, 2496 (1993).

14. O. Züger and D. Rugar, J. Appl. Pliys. 75, 6211 (1994).

15. O. Zuger, S. T. Hoen, C. S. Yannoni and D. Rugar, J. Appl. Pliys. (1996), to be published.

16. D. Rugar, O. Zuger, S. Boeii, C. S. Yannoni, H.-M. Vieth and R.D. Kendrick, Science 264, 1560 (1994).

17. In a private commuiiication (C. Frediani), it was brought to our attention tliat ESR lias been detected by measuring tlie torque iii a mechanical oscillator: see G. Alzetta, E. Arimondo, C. Ascoli ancl A. Gozzini, Nuovo Ciinento 52B, 392 (1967).

18. A large (millimeter-size) magnetic tip was used in order to ensure tliat tlie resonant volume was large enough, i.e. contained a sufficient number of spins, to generate a measurable signal. In the NMR experiment on ammonium nitrate, for example, tlie force noise was such tliat tlie minimum detectable inagnetic moment in a field of 2.5T at 300K corresponded to 1.6×10^{13} protons, a sample 1 μm thick by 20 μm square[16]. Tliis required an iron tip far too large to attach to tlie 50 μm-long cantilever. In general, as tlie tip size ancl tlie spacing between tip and sample are scaled to smaller dimensions, tlie gradient increases iii inverse proportion to tlie scale factor. Tliis has tlie beneficial effect of increasing tlie force per spin (or force per unit volume). However, the volume of resonant spins decreases faster as tlie dimensions are scaled down, resulting in a netreduction of force for most sainple geometries. These comments obviously do not apply to tlie case of single-spin MRFM, for which tlie gradient may be increasecl witliout concern for tlie size of the resonant volume.

19. S. Hoen, O. Zuger, C. S. Yannoni, H. J. Mamin, K. Wago, and D. Rugar, In 7YY4 *Solid-state sensor and actuator workshop technical* digest (Transducer Research Foundation, Cleveland Height, 1994) p. 209.

20. D. Rugar, C. S. Yannoni and J. A. Sidles, Nature 360, 563 (1992).

21. G. Whitfield aiid A. G. Redfield, Phys. Rev. 106, 918 (1957).

22. K. J. Bruland, J. Krzystek, J. L. Garbini and J. A. Sidles, Rev. Sci. Instrum. 66, 2853 (1995).

23. Tlie cantilevers are commercially availahle from Park Scientific Instruments, Sunnyvale, California, or Digital Instruments Inc., Santa Barbara, California.

24. A. Abragam, *The Principles of Nuclear Magnetism* (Oxford Uiiiversity Press, London, 1961), pp. 65 ancl 545-548.

25. J. A. Siclles suggested cyclic acliabatic inversion as a means to create a slowly oscillating nuclear magnetic moment (personal commuiiication).

26. O. Zuger, S. T. Hoen, H.-M. Vieth, C. S. Yannoni and D. Rugar (in preparation).

27. For a review of solid state NMR imaging, see e.g., D.G. Cory, in Aiinual Reports on NMR Spectroscopy, editecl by G. A. Webb (Academic, London, 1992), Vol. 24, p.87.

28. P. T. Callaghan, *Principles of Nuclear Magnetic Resonance Microscopy* (Clarendon Press, Oxford, 1991), p. 192.

29. K. Wago, O. Zuger, R. Kendrick, C. S. Yannoni ancl D. Rugar, J. Vac. Sci. ancl Tech., to be publisliecl (1996).

30. C. V. Heer, Statistical *Mechanics, Kinetic Theory,* and *Stochastic* Processes (Academic, New York, 1972), p. 431.

31. J. A. Sidles ancl D. Rugar, Phys. Rev. Lett. 70, 3506 (1993).